ChemComm

Accepted Manuscript

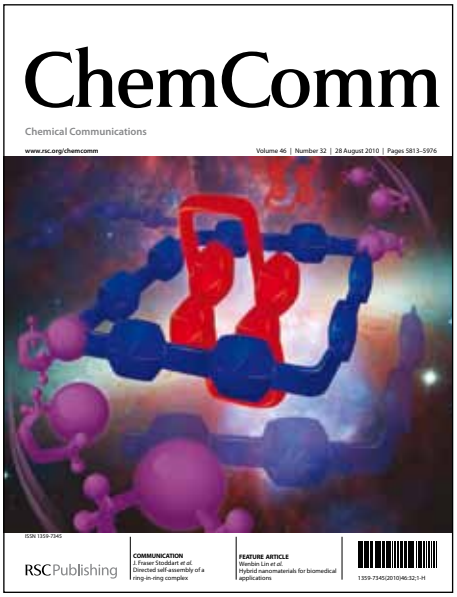

This is an *Accepted Manuscript*, which has been through the RSC Publishing peer review process and has been accepted for publication.

Accepted Manuscripts are published online shortly after acceptance, which is prior to technical editing, formatting and proof reading. This free service from RSC Publishing allows authors to make their results available to the community, in citable form, before publication of the edited article. This *Accepted Manuscript* will be replaced by the edited and formatted *Advance Article* as soon as this is available.

To cite this manuscript please use its permanent Digital Object Identifier (DOI®), which is identical for all formats of publication.

More information about *Accepted Manuscripts* can be found in the **Information for Authors**.

Please note that technical editing may introduce minor changes to the text and/or graphics contained in the manuscript submitted by the author(s) which may alter content, and that the standard **Terms & Conditions** and the **ethical guidelines** that apply to the journal are still applicable. In no event shall the RSC be held responsible for any errors or omissions in these *Accepted Manuscript* manuscripts or any consequences arising from the use of any information contained in them.

Journal Name

RSCPublishing

COMMUNICATION

Cite this: DOI: 10.1039/x0xx00000x

Two- and one-step cooperative spin transitions in Hofmann-like clathrates with enhanced loading capacity

Received 00th January 2012,
Accepted 00th January 2012

DOI: 10.1039/x0xx00000x

www.rsc.org/

Lucía Piñeiro-López,[a] Maksym Seredyuk,[a,b] M. Carmen Muñoz,[c] José A. Real*[a]

Structural, magnetic, calorimetric and Mössbauer studies of the cooperative spin crossover naphthalene and nitrobenzene clathrates of the novel Fe^{II} Hofmann-like porous metal-organic framework {Fe(*bpb*)[Pt(CN)$_4$]}·2Guest are described (*bpb* = bis(4-pyridyl)butadiyne).

Porous three-dimensional (3D) metal-organic frameworks (PMOFs) exhibit useful physical properties such as electrical and hydrogen conductivity,[1] storage,[2] luminescence,[3] catalysis[4] and separation.[5] PMOFs provide synthetic accessibility, chemical robustness and ease modification to meet particular practical demands. Furthermore, they can offer tunable physical properties if prepared from bistable building blocks. Indeed, in the case of PMOFs based on $3d^6$ Fe^{II} ions, the spin crossover (SCO) phenomenon can be observed with reversible switch between the diamagnetic low-spin (LS, S = 0) and the paramagnetic high-spin (HS, S = 2) states involving magnetic, optical, and structural changes in response to the change of temperature, pressure, or light irradiation.[6] It is well known that SCO characteristics (critical temperature, abruptness, completeness) are related to the chemical nature of the ligands coordinated to the Fe^{II} ion, however, they are also greatly influenced by crystal packing effects, particularly, exerted by non-coordinated inclusions (anions, solvents and guest molecules).[7] Particularly, the sensitivity of SCO in Fe^{II} PMOFs toward the guest molecules confers sensory function to the materials and makes them attractive from the viewpoint of the possible practical application as sensors.

Cyanide-bridged Fe^{II}–M^{II} (M = Ni, Pd, Pt) bimetallic 3D networks, also known as Hofmann-like PMOFs, represent an example of materials with exceptionally abrupt hysteretic SCO and capability to sense guest molecules. Generically formulated {Fe(L)[M^{II}(CN)$_4$]}·G they have been reported for L = *pz*,[8-10] *azpy*,[11] *dpe*,[12] bpe,[13] *bpac*,[14,15] *dpmse*[16] or *bpeben*[17] (Scheme I). These SCO-PMOFs possess both, accessible voids responsible for the uptake of guest molecules by the framework and, coordinatively unsaturated M^{II} centres able to give oxidative addition of halogens.[10] Further development of SCO-PMOFs is guided toward increasing the pore size and pore functionality. Here we report the synthesis and characterization of two Fe^{II}

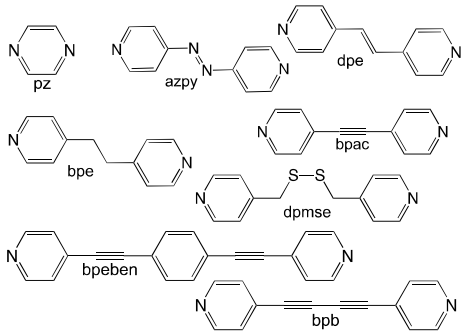

Scheme I. Pillar ligands for {Fe(L)[M^{II}(CN)$_4$]}·G Hofmann-like PMOFs.

Hofmann-like 3D clathrates of the unprecedented SCO-PMOF {Fe(*bpb*)[Pt(CN)$_4$]}·2G [G is naphthalene (**1**) or nitrobenzene (**2**)] based on the elongated ditopic ligand bis(4-pyridyl)butadiyne (*bpb*, Scheme I). These clathrates exhibit cooperative SCO and, to the best of our knowledge, this new MOF system shows the highest load capacity reported up to now.

Both clathrates were synthesised by slow diffusion in multiarm-shaped vessels (see synthesis and Figures S1 and S2 in ESI). They are isostructural and adopt the general topology of 3D {FeL[M(CN)$_4$)]} PMOFs consisting of infinite two-dimensional {Fe[Pt(CN)$_4$]}$_\infty$ layers bridged by pillaring ligands through axially coordinated Fe^{II} ions (Fig. 1). However, in contrast to the rest members of the {FeL[M(CN)$_4$)]} series, **1** and **2** crystallize in the triclinic $P\bar{1}$ space group. The crystallographic parameters for both compounds are collected in Table S1, and selected angles and distances in Tables S2, S3 (ESI). The ligand *bpb* adopts a markedly bent conformation in contrast to other unsaturated bridging ligands mentioned above

and, additionally, the pyridine moieties locate practically perpendicular to each other. Similar geometries were observed in the triply interlocked catenane SCO $[Fe(bpb)_2(NCS)_2]\cdot 1/2MeOH$ complex.[18] Due to the curvature shown by the *bpb* ligand, the axially elongated FeN_6 octahedrons are alternatively tilted, within de *bc* plane, in opposite directions thereby conferring to the $\{Fe[Pt(CN)_4]\}_\infty$ layers a corrugated geometry.

Two guest molecules per unit cell are found in **1** and **2**. One is located half-way between the pyridine rings of the *bpb* ligand, which coordinate to Fe(1), while the second lies closer to the pyridine ring coordinated to Fe(2) (see Fig. 1 and Fig. S3). There are numerous C···C contacts between the guest molecules and the pyridine rings changing with temperature according to expansion/contraction of the lattice due to the SCO of the Fe^{II} ions (Table S4, ESI). These contacts influence in a different way on the coordination spheres the two Fe^{II} ions. Indeed, the averaged bond length <Fe–N> (vide infra) is slightly different for Fe(1) and Fe(2). For **1**, <Fe(1)–N> changes from 2.13(2) Å at 250 K to 1.957(2) Å at 195 K and further remains constant upon cooling to 120 K (1.959(5) Å) where the complete transition to the LS state takes place. At 250 K, the value <Fe(2)–N> is 2.14(2) Å and does not vary much upon cooling to 195 K (2.160(2) Å), but decreases to 1.966(5) Å at 120 K. Evidently, Fe(1) undergoes transition above 195 K, while Fe(2) below this temperature. For **2**, <Fe(1)–N> changes from 2.175(12) Å at 250 K to 1.955(5) Å at 120 K and for <Fe(2)–N> from 2.175(11) Å at 250 K to 1.956(5) Å at 120 K. The transition of both Fe^{II} ions takes place simultaneously.

There are two different types of pores running respectively along *a* and *b* axes hosting the guest molecules. The pores running along *a* are much wider than those running along *b* due to the bent shape of *bpb*. The cross-section of the expanded pores, defined by Fe···Fe distances through the bent ligand *bpb* and the corrugated $[Pt(CN)_4]^{2-}$ anions, makes *ca*. 15.87(1) Å × 6.98(1) Å at 120 K. The accessible volume[19] of the frameworks **1** (**2**) (without considering guest molecules) is 849.6 (801.8) $Å^3$ and

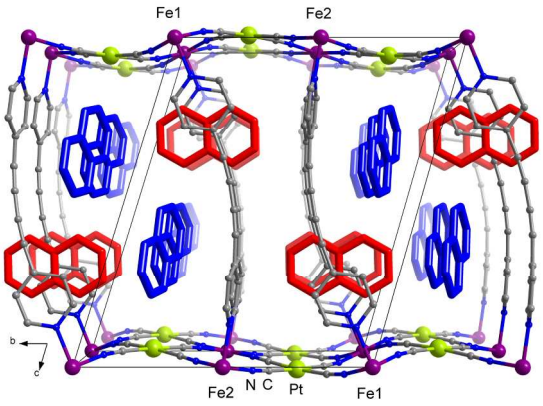

Fig. 1. Projection of the structure of **1** along *a*. Two types of guest naphthalene molecules are coloured in red and blue.

corresponds to 53.8 % (52.6%) of the unit cell volume at 120 K (1579.2 $Å^3$ (**1**) and 1523.3 $Å^3$ (**2**)). The porosity of the frameworks in **1** and **2** is larger in comparison with that found for SCO clathrates $\{FeL[Pt(CN)_4]\}$, which is 22 % for *pz*, *ca*. 40 % for *azpy*,[11] *dpe*[12] and *bpac*[15] and 48% for *bpeben*.[17]

Fig. 2 displays the magnetic and calorimetric properties of **1** and **2**. At 300 K, the $\chi_M T$ product (χ_M is the molar magnetic susceptibility and T is temperature) is ca. 3.5–3.6 $cm^3\ K\ mol^{-1}$ and remains constant until approaching the SCO transition. In the case of **1**, the Fe^{II} ions undergo transition in two equal steps at $T_{c1}{}^{\downarrow}$ = 205 K and $T_{c2}{}^{\downarrow}$ = 188 K. Upon heating, the critical temperatures are $T_{c2}{}^{\uparrow}$ = 203 K and $T_{c1}{}^{\uparrow}$ = 216 K defining two hysteresis loops of 15 K and 11 K width, respectively. In **2**, the transition takes place in one step with $T_c{}^{\downarrow}$ = 210 K and $T_c{}^{\uparrow}$ = 237 K with the hysteresis loop 27 K wide. In the low temperature region the $\chi_M T$ values are near to zero.

The calorimetric measurements performed on samples of **1** and **2** in the anomalous heat capacity ΔC_p vs T are shown in Fig. 2. The enthalpy (ΔH) and entropy (ΔS) average variations associated with the spin transitions are: ΔH = 9.45 kJ mol^{-1} and ΔS = 44.9 J K^{-1} mol^{-1} for the high temperature hysteresis loop and ΔH = 8.62 kJ mol^{-1} and ΔS = 44.1 J K^{-1} mol^{-1} for the low temperature hysteresis loop of **1**; ΔH = 19.29 kJ mol^{-1} and ΔS = 86.3 J K^{-1} mol^{-1} for **2**. These values are typical for cooperative SCO in Hofmann-like clathrates of Fe^{II}.[6c]

Fig. 2. Magnetic (filled circles) and calorimetric (blue and red lines refer to cooling and heating modes, respectively) measurements for **1** (left) and **2** (right).

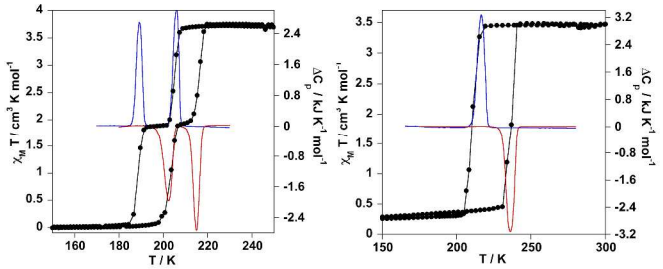

The Mössbauer spectrum of **1** at 80 K consist of two LS doublets with almost identical isomer shift values (δ^{LS1} = 0.47(2) mm s^{-1} and δ^{LS2} = 0.49(2) mm s^{-1}) and different quadrupole splitting parameters ($\Delta E_Q{}^{LS1}$ = 0.32(1) mm s^{-1} and $\Delta E_Q{}^{LS2}$ = 0.16(2) mm s^{-1}) (Fig. 3 left). The relative areas A of the two doublets have ratio close to 1:1. Evidently, the doublets correspond to two different Fe^{II} sites observed in the crystal lattice of the compound. Upon increasing the temperature to 199 K and according to the transition of one of the Fe^{II}-sites to the HS state, in the spectrum disappears a LS doublet and instead a HS doublet is detected (δ^{HS} = 1.11(2) mm s^{-1} and $\Delta E_Q{}^{HS}$ = 1.53(4) mm s^{-1}). The parameters of the second LS doublet remains at this temperature almost unchanged (δ^{LS} = 0.47(1) mm s^{-1} and $\Delta E_Q{}^{LS}$ = 0.14(3) mm s^{-1}). Upon heating to 300 K, the spectrum of **1** contains two overlapping equally populated HS doublets with similar isomer shift values (δ^{LS1} = 1.05(1) mm s^{-1} and δ^{HS2} = 1.06(1) mm s^{-1}) and strongly different quadrupole splitting parameters ($\Delta E_Q{}^{HS1}$ = 0.51(2) mm s^{-1} and $\Delta E_Q{}^{HS2}$ = 1.21(2) mm s^{-1}). The ΔE_Q values reflect

different geometric distortion of the corresponding coordination polyhedrons. The spectra of **2** collected at 80 and 300 K in the

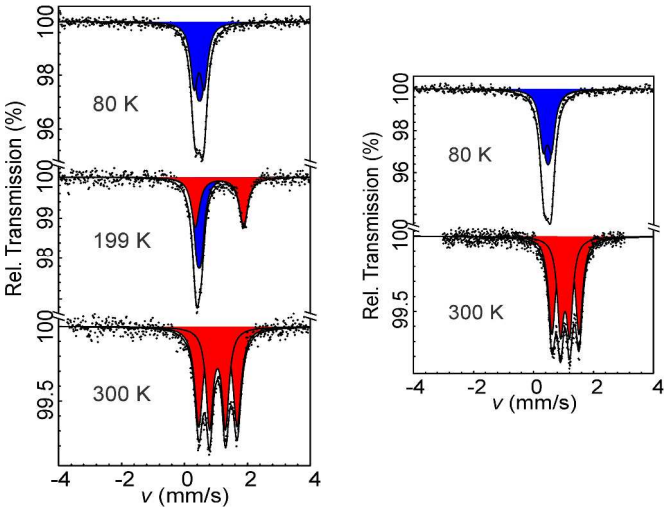

Fig. 3. Mössbauer spectra for **1** (left) and **2** (right). Red and blue colours represent the HS and LS components of the spectra.

LS and HS states, respectively, are very similar to those of **1** at the same temperatures (Fig. 3 right; Table S6, ESI).

In conclusion we have reported the synthesis, structure, spectroscopic and magnetic characterization of a new type of Hofmann-like SCO-MOFs exhibiting large thermal hysteresis and the largest effective porosity among up to now reported Hofmann-like SCO-PMOFs. The compounds display distinguishable magnetic behaviour related to the absorbed analyte that confers to the magnetic response an identifying characteristic. Extended studies of the structure–property relationship of these materials are in progress.

The Spanish MINECO, FEDER (CTQ2010-18414) and the GV (PROMETEO/2012/049) are thanked for funding. MS thanks the EU for a Marie Curie fellowship (IIF-253254). LPL thanks the GV for a pre-doctoral fellowship. We acknowledge Prof. P. Gütlich and Dr. V. Ksenofontov from the University of Mainz (Germany) for providing access to Mössbauer spectrometers.

Notes and references

[a]Institut de Ciència Molecular (ICMol), Departament de Química Inorgànica, Universitat de València, C/ Catedrático José Beltrán Martínez, 2, 46980 Paterna (Valencia), Spain e-mail: jose.a.real@uv.es.

[b] Permanent address: Taras Shevchenko National University, Department of Physical Chemistry, Volodymyrska Str. 64, Kyiv 01601, Ukraine.

[c] Departament de Física Aplicada, Universitat Politècnica de València, Camino de Vera s/n, 46022, Valencia, Spain.

Electronic Supplementary Information (ESI) available: Experimental procedures, thermogravimetric analyses (Figure S1), Infrared spectra (Figure S2), crystallographic data (Tables S1-S5), Mössbauer data (Table S6) and projection of the structure 2 along *a* (Figure S3). CCDC 971021-971025. See DOI: 10.1039/c000000x/

1. a) M. Yoon, K. Suh, S. Natarajan and K. Kim, *Angew. Chem., Int. Ed.*, 2013, **52**, 2688-2700; b) A. Morozan and F. Jaouen, *Energy & Environmental Science*, 2012, **5**, 9269-9290.
2. a) M. P. Suh, H. J. Park, T. K. Prasad and D.-W. Lim, *Chem. Rev.*, 2012, **112**, 782-835; b) T. A. Makal, J.-R. Li, W. Lu and H.-C. Zhou, *Chem. Soc. Rev.*, 2012, **41**, 7761.
3. J. Rocha, L. D. Carlos, F. A. A. Paz and D. Ananias, *Chem. Soc. Rev.*, 2011, **40**, 926.
4. M. Yoon, R. Srirambalaji and K. Kim, *Chem. Rev.*, 2012, **112**, 1196-1231; L. Ma and W. Lin, 2009, **293**, 175-205.
5. a) Y. Yu, Y. Ren, W. Shen, H. Deng and Z. Gao, *TrAC Trends in Analytical Chemistry*, 2013, **50**, 33-41; b) J.-R. Li, J. Sculley and H.-C. Zhou, *Chem. Rev.*, 2012, **112**, 869-932.
6. a) P. Gütlich and G. Goodwin (eds.), *Top. Curr. Chem.*, 2004, **233, 234, 235**; b) A. B. Gaspar, V. Ksenofontov, M. Seredyuk and P. Gütlich, *Coord. Chem. Rev.*, 2005, **249**, 2661-2676; c) M. C. Muñoz and J. A. Real, *Coord. Chem. Rev.*, 2011, **255**, 2068-2093; d) M. A. Halcrow (ed.), *Spin-Crossover Materials: Properties and applications*, John Wiley & Sons Ltd, 2013.
7. P. Gütlich and H. A. Goodwin, *Top. Curr. Chem.*, 2004, **233**, 1-47.
8. V. Niel, J. M. Martinez-Agudo, M. C. Muñoz, A. B. Gaspar and J. A. Real, *Inorg. Chem.*, 2001, **40**, 3838-3839.
9. a) M. Ohba, K. Yoneda, G. Agusí, M. C. Munoz, A. B. Gaspar, J. A. Real, M. Yamasaki, H. Ando, Y. Nakao, S. Sakaki and S. Kitagawa, *Angew. Chem., Int. Ed.*, 2009, **48**, 4767-4771; b) P. D. Southon, L. Liu, E. A. Fellows, D. J. Price, G. J. Halder, K. W. Chapman, B. Moubaraki, K. S. Murray, J.-F. Letard and C. J. Kepert, *J. Am. Chem. Soc.*, 2009, **130**, 10998-11009.
10. G. Agusti, R. Ohtani, K. Yoneda, A. B. Gaspar, M. Ohba, J. F. Sanchez-Royo, M. C. Munoz, S. Kitagawa and J. A. Real, *Angew. Chem., Int. Ed.*, 2009, **48**, 8944-8947.
11. G. Agustí, S. Cobo, A. B. Gaspar, G. Molnar, N. O. Moussa, P. A. Szilagyi, V. Palfi, C. Vieu, M. C. Muñoz, J. A. Real and A. Bousseksou, *Chem. Mater.*, 2008, **20**, 6721-6732.
12. F. J. Muñoz-Lara, A. B. Gaspar, M. C. Muñoz, M. Arai, S. Kitagawa, M. Ohba and J. A. Real, *Chemistry – A European Journal*, 2012, **18**, 8013-8018.
13. R. Ohtani, M. Arai, A. Hori, M. Takata, S. Kitao, M. Seto, S. Kitagawa and M. Ohba, *J. Inorg. Organomet. Polym. Mater.*, 2013, **23**, 104-110.
14. C. Bartual-Murgui, L. Salmon, A. Akou, N. A. Ortega-Villar, H. J. Shepherd, M. C. Muñoz, G. Molnár, J. A. Real and A. Bousseksou, *Chem. Eur. J*, 2012, **18**, 507-516.
15. C. Bartual-Murgui, N. A. Ortega-Villar, H. J. Shepherd, M. C. Muñoz, L. Salmon, G. Molnár, A. Bousseksou and J. A. Real, *J. Mater. Chem.*, 2011, **21**, 7217.
16. N. F. Sciortino, K. R. Scherl-Gruenwald, G. Chastanet, G. J. Halder, K. W. Chapman, J.-F. Létard and C. J. Kepert, *Angew. Chem., Int. Ed.*, 2012, **51**, 10154-10158.
17. F. J. Muñoz-Lara, A. B. Gaspar, M. C. Muñoz, V. Ksenofontov and J. A. Real, *Inorg. Chem.*, 2012, **52**, 3-5.
18. N. Moliner, C. Muñoz, S. Létard, X. Solans, N. Menéndez, A. Goujon, F. Varret, J. A. Real, Inorg. Chem. 2000, 39, 5390-5393.
19. A. Spek, *Acta Crystallographica Section D*, 2009, **65**, 148-155.